MOLECULAR AND CELLULAR BIOLOGY, Mar. 2005, p. 1669–1679 Vol. 25, No. 5
0270-7306/05/$08.00+0 doi:10.1128/MCB.25.5.1669–1679.2005

Dap1p, a Heme-Binding Protein That Regulates the Cytochrome P450 Protein Erg11p/Cyp51p in *Saccharomyces cerevisiae*

Julia C. Mallory,[1] Gerard Crudden,[1] Ben L. Johnson,[1] Caiqing Mo,[2] Charles A. Pierson,[2] Martin Bard,[2] and Rolf J. Craven[1]*

Department of Molecular and Biomedical Pharmacology, Markey Cancer Center, University of Kentucky, Lexington,[1] Kentucky, and Department of Biology, Indiana University—Purdue University at Indianapolis, Indianapolis, Indiana[2]

Received 17 August 2004/Returned for modification 4 October 2004/Accepted 29 November 2004

Alkylating agents chemically modify DNA and cause mutations that lead to cancer. In the budding yeast *Saccharomyces cerevisiae*, resistance to the alkylating agent methyl methanesulfonate (MMS) is mediated in part by Dap1p (damage resistance protein 1). Dap1p is related to cytochrome b_5, which activates cytochrome P450 proteins, elevating the metabolism of lipids and xenobiotic compounds. We have found that Dap1p, like cytochrome b_5, binds to heme and that Dap1p targets the cytochrome P450 protein Erg11p/Cyp51p. Genetic analysis indicates that Erg11p acts downstream of Dap1p. Furthermore, Dap1p regulates the stability of Erg11p, and Erg11p is stabilized in *dap1*Δ cells by the addition of heme. Thus, Dap1p utilizes heme to stabilize Erg11p, which in turn regulates ergosterol synthesis and MMS resistance. Dap1p homologues have been identified in numerous eukaryotes, including mammals, suggesting that the Dap1p-cytochrome P450 protein pathway is broadly conserved in eukaryotic species.

Alkylating agents are produced industrially and are common environmental pollutants and carcinogens. Alkylating agents such as cyclophosphamide, cisplatin, and busulfan are used to treat cancer because they induce DNA breaks (15). While the mechanism of action of alkylating agents is established, the genes that mediate cellular resistance to these agents are less well understood. The budding yeast *Saccharomyces cerevisiae* is a model organism for analyzing responses to alkylating agents. The methylating agent methyl methanesulfonate (MMS) is widely used in yeast for mutagenesis and damage repair studies (9), because MMS causes various types of genomic instability (26, 28). MMS triggers a broad transcriptional response in yeast (10, 17), and approximately 100 genes are required for resistance to MMS (3, 4, 5). Because of the importance of alkylating agents in carcinogenesis and in the treatment of cancer, there is increasing interest in the genes that regulate cellular responses to these agents.

Dap1p (damage resistance protein 1) is required for resistance to MMS in *S. cerevisiae* (3, 14). Dap1p is a predicted 25-kDa protein comprised largely of a heme-1 domain, a region of homology with cytochrome b_5 (22). Cytochrome b_5 is a heme-binding protein that positively regulates some reactions catalyzed by cytochrome P450 proteins (30). Cytochrome P450 proteins inactivate a broad spectrum of hormones and xenobiotic compounds and drive key steps in lipid metabolism (27, 37). P450 proteins require a reductase, and cytochrome b_5 can increase the efficiency of P450-mediated reactions by acting as a primary or secondary electron donor (20). Dap1p resembles cytochrome b_5 structurally, and the rat and human homologues of Dap1p bind to heme (24; G. Crudden and R. J. Craven, unpublished observations). Homologues of Dap1p have been detected in numerous eukaryotes, including human (11), porcine (22), rat (29, 31), and murine (19) homologues, as well as related genes that have yet to be characterized in fission yeast, flowering plants, *Drosophila melanogaster*, and *Caenorhabditis elegans* (14).

We previously demonstrated that Dap1p is required for resistance to DNA damage from MMS (14), and this finding was duplicated by Begley et al. by using a large-scale genomic screen (3). While *dap1*Δ mutants exhibit stronger sensitivity to MMS than wild-type strains (14), they are only moderately sensitive to hydroxyurea (14) and are not sensitive to UV irradiation or 4-nitroquinoline-*N*-oxide (3). In contrast, *dap1*Δ mutants are moderately resistant to *tert*-butyl hydroperoxide (3). Thus, Dap1p mediates resistance to a relatively narrow range of damaging agents, and Dap1p has the strongest activity towards the methylating agent MMS.

Cells lacking Dap1p demonstrate a partial arrest in sterol synthesis (14). We found that *dap1*Δ mutants accumulate the ergosterol synthetic intermediates squalene and lanosterol while synthesizing decreased amounts of the metabolic products of lanosterol (Fig. 1) (14). Erg11p/Cyp51p is a lanosterol demethylase (Fig. 1), and Erg11p/Cyp51p catalyzes the conversion of lanosterol to its metabolite 4,4-dimethylcholesta-8,14,24-trienol (7). The analysis of sterols in *dap1*Δ cells indicates a defect in the step catalyzed by Erg11p, suggesting that Dap1p activates Erg11p. Furthermore, *dap1*Δ mutants are sensitive to the antifungal agents itraconazole and fluconazole (14), which are direct inhibitors of the Erg11p enzyme (Fig. 1) (34).

The sterol synthetic defects in *dap1*Δ mutants suggest that *dap1*Δ mutants might be sensitive to MMS due to porous cell membranes that could allow for an elevated accumulation of the agent. However, *dap1*Δ mutants have a slightly defective uptake of crystal violet (14), a marker for membrane integrity,

* Corresponding author. Mailing address: Department of Molecular and Biomedical Pharmacology, University of Kentucky, MS-305 UKMC, Lexington, KY 40536. Phone: (859) 323-3832. Fax: (859) 257-9608. E-mail: rolf.craven@uky.edu.

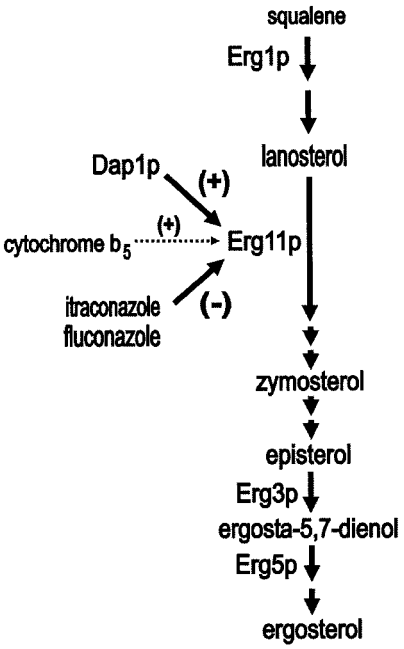

FIG. 1. The sterol biosynthetic pathway in yeast. Following conversion of acetyl coenzyme A to squalene (7), the later stages of ergosterol synthesis convert squalene to the final product of the pathway, ergosterol. A key step in this process, the demethylation of lanosterol, is catalyzed by Erg11p. Erg11p is the target of the antifungal drugs itraconazole and fluconazole, and earlier work by Hand et al. (14) suggested that Dap1p also targets Erg11p. Cyb5p also contributes to Erg11p activation in vitro (20) (dashed line). In *dap1*Δ mutants, squalene and lanosterol are elevated while zymosterol is decreased (14). In addition, *dap1*Δ mutants are sensitive to itraconazole (14). Episterol and ergosta-5,7-dienol are downstream metabolites of lanosterol.

and *dap1*Δ mutants are not sensitive to a cation pulse, another test for membrane integrity (14). In contrast, other ergosterol synthetic mutants have marked increases in crystal violet uptake and are sensitive to a cation pulse (2). The narrow range of compounds to which Dap1p mediates resistance also argues against a general membrane defect in *dap1*Δ cells, and *dap1*Δ mutants are moderately resistant to some damaging agents (3).

In the present study, we show that Dap1p, like its mammalian homologues, is a heme-binding protein and that a point mutation within the heme-1 domain abolishes heme binding and confers damage sensitivity. We also demonstrate that Dap1p targets Erg11p in sterol biosynthesis and damage resistance, because *ERG11* is a multicopy suppressor of *dap1*Δ phenotypes. Finally, we show that Dap1p regulates Erg11p by maintaining Erg11p levels. Erg11p is clinically important as a target for antifungal agents, and we have demonstrated a novel role for Erg11p in damage resistance. These findings suggest that Dap1p is a promising therapeutic target, both in antifungal chemotherapy and as a model for chemotherapeutic resistance in mammalian cells.

MATERIALS AND METHODS

Yeast strains and growth conditions. All strains were isogenic with W303 (*leu2-3,112 his3-11,15 ura3-1 ade2-1 trp1-1 can1-100 rad5-535*) (32). For the strains used in this study, the *rad5-535* allele was replaced with the wild-type *RAD5* gene by crossing and was tested by PCR as described elsewhere (6). All genetic manipulations and transformations with plasmid DNA were performed as previously described (13). The yeast strains RCY407-12d and RCY409-2a (both wild type) and RCY407-1d and RCY409-4b (both *dap1*Δ*::LEU2*) have been described previously (14). The *erg2*Δ strain JRY7187 was a gift from Jasper Rine's laboratory.

Plasmids. The plasmids used in this study are summarized in Table 1. The *ERG11* gene was amplified using the primers *ERG11*-300F-Hind and *ERG11*+1650R-Bam. The sequences of all primers used in this study are available at the website www2.mc.uky.edu/Pharmacology/rjc_research.asp. The PCR product was digested with HindIII and BamHI and ligated to the plasmid YEp*lac*195 (12), which was digested with the same enzymes. The resulting plasmid (called pRH4) contained the entire *ERG11* open reading frame, along with 300 bp of its upstream sequence. The *ERG1* gene was amplified by PCR using the primers *ERG1*-290F-Bam and *ERG1*+1524R-Hind, and the resulting PCR product was subcloned into the plasmid YEp*lac*195, forming the plasmid pJM60.

For epitope tagging the *ERG11* open reading frame, the entire *ERG11* gene was amplified using W303a genomic DNA as a template with the primers *ERG11*-300F-Hind and *ERG11*+1650-MYCR-Bam. The PCR product was digested with BamHI and HindIII and cloned into the corresponding sites of the single-copy plasmid pRS316. The resulting plasmid was called pRH7.

For *DAP1* mutagenesis, *DAP1* was amplified by PCR using the primers DAP-200F and DAP+470R and subcloned into the plasmid pCR3.1 (Invitrogen), forming the plasmid pRC31. The Dap1p-D91G mutation was created with the ExCite mutagenesis kit (Stratagene) using the manufacturer's instructions and the primers *DAP1*-D91G-F and *DAP1*+265R with pRC31 as a template, forming the plasmid pRC34. After confirming the integrity of the D91G mutation, the *DAP1*-D91G mutant was subcloned into the XhoI and EcoRI sites of the plasmid pRS313, forming the plasmid pRC39. The wild-type gene was similarly cloned into pRS313, forming the plasmid pRC41.

For production of a Dap1p fusion protein with glutathione *S*-transferase, the *DAP1* open reading frame from bp 4 to 459 was amplified by PCR using the primers *DAP1*+4F-Bgl and *DAP1*+457R-Xho, with W303a genomic DNA as a template. The PCR product was then subcloned into the BamHI and XhoI sites of the plasmid pGEX-4T-1 (Amersham), forming the plasmid pGC5. The *DAP1*-D91G mutant was subcloned similarly. To construct the plasmid encoding the Dap1p protein containing the D91G mutation, the mutated *DAP1* open reading frame was amplified using the same primers with pRC34 as a template and subcloned into the same sites of pGEX-4T-1. The resulting plasmid was called pGC4. The sequences of all cloned genes were confirmed by automated sequenc-

TABLE 1. Plasmids used in this study

Name	Core plasmid	Insert
pGC5	pGEX-4T-1	*DAP1* ORF, bp 4 to 459
pGC4	pGEX-4T-1	*DAP1* ORF, bp 4 to 459 containing the D91G mutation
pJM60/YEp-*ERG1*	YEp*lac*195	*ERG1* ORF with 290 bp of 5′ genomic sequence
pRC31	pCR3.1	*DAP1* ORF with 200 bp of 5′ genomic sequence
pRC34	pCR3.1	pRC31 mutated to *DAP1*^{D91G}
pRC39/*DAP1*^{D91G}-CEN	pRS313	*DAP1* ORF with 200 bp of 5′ sequence and the D91G mutation
pRC41/*DAP1*-CEN	pRS313	*DAP1* ORF with 200 bp of 5′ sequence
pRH4/YEp-*ERG11*	YEp*lac*195	*ERG11* ORF with 300 bp of 5′ genomic sequence
pRH7	pRS316	*ERG11* ORF with 300 bp of 5′ sequence and a single carboxy-terminal Myc epitope tag

ing using core facilities at the University of North Carolina at Chapel Hill and the University of Cincinnati.

Fusion protein purification and measurement of heme binding. Bacteria harboring the pGC4 and pGC5 plasmids were grown to an A_{600} of 0.3, treated with isopropyl-β-D-thiogalactopyranoside for 4 h, and collected by centrifugation. Bacteria were lysed by incubation in the B-PER reagent (Pierce) and bound to glutathione-agarose columns for 2 to 20 h at 4°C. The columns were then washed three times with phosphate-buffered saline. A 100-μg aliquot of fusion protein was liberated with 1 U of thrombin (Fisher) by incubation at 37°C for 2 h with agitation. The glutathione-agarose column was then removed by centrifugation, and the A_{400} of the supernatant was measured in a microtiter plate reader. Measurements were performed in triplicate using three separate aliquots of fusion protein. At the onset of the experiment, the absorption spectrum from 300 to 700 nm for Dap1p was determined using a Spectronics Genesys 5 spectrophotometer (Spectronics Instruments), before and after the addition of 0.5 mg of sodium dithionate (a kind gift of Todd Porter, originally from Sigma).

Growth assays. The ability of various strains to grow on itraconazole and MMS was determined using a spotting assay as previously described (14). Briefly, overnight cultures were serially diluted 1:10 and spotted on plates lacking histidine or uracil, as indicated in the figure legends. Where indicated, plates also contained 0.01 to 0.015% MMS (Sigma) or were overlaid with 0.2 mg of itraconazole (Ortho Biotech)/ml. For some experiments, 13 μg of hemin (Sigma; diluted from a 1.3-mg/ml stock in 50% ethanol and 0.1 N NaOH in water)/ml was added to the plates prior to testing viability. Before performing the spotting assay, yeast strains were maintained for 3 to 5 days on yeast extract-peptone-dextrose (YPD) plates containing 13 μg of hemin/ml to ensure uptake of heme.

To calculate 50% lethal dose (LD_{50}) values, liquid yeast cultures were grown overnight and then diluted to an A_{600} of 0.1, and 50 μl of diluted culture was added to a 96-well culture dish. An additional 50 μl of medium containing 0 to 0.016% MMS was then added to each well, and the cells were grown at 30°C with shaking until the A_{600} of cells that were not treated with MMS reached 0.5. The A_{600} of all of the wells was then measured using a Thermo Lab System Multi-Scan MCC/340 microtiter plate reader. The effect of each dose of MMS on each strain was measured in triplicate, and the LD_{50} was calculated using Microsoft Excel. The standard deviation of three independent measurements was compared for the separate strains. To validate the assay, we calculated the LD_{50} values for wild-type (RCY409-2a), *dap1*Δ (RCY409-4b), and *dun1*Δ (RCY144-1a) strains. The LD_{50} for the wild-type strain was 0.013% MMS, while the LD_{50} for *dap1*Δ was 0.005% and for *dun1*Δ it was 0.003%. The difference between wild-type and *dap1*Δ strains was highly significant ($P = 0.0004$; t test).

Sterol analysis. Sterol profiles were analyzed using the KOH–*n*-heptane extraction procedure of Molzahn and Woods (25) as previously described (14). Cells were grown in liquid medium and harvested for sterol analysis at an A_{600} of 0.8. Cells were pelleted, washed once with distilled water (dH_2O), and resuspended in 4.5 M KOH–60% ethanol. Cells were then refluxed in a round-bottom flask at 88 to 90°C for 1 h. A 95% ethanol solution was then added, and the cells were refluxed for an additional hour and then cooled to room temperature. The mixture was then extracted with *n*-heptane and dH_2O, and the *n*-heptane layer was analyzed by gas chromatography. Each sample was injected twice, and a representative profile is shown. Sterols were analyzed by gas chromatography with a Hewlett-Packard HP5890 series II chromatograph as described elsewhere (14). In some cases, cells were pregrown for 50 generations on YPD plates containing 13 μg of hemin/ml and then grown in liquid YPD containing hemin for sterol analysis.

Protein analysis. Yeast cells were diluted and grown to early log phase, then centrifuged, washed once with water, and lysed by incubation in the Y-PER reagent (Pierce) containing 1 mM phenylmethylsulfonyl fluoride and 10 μg of the protease inhibitors aprotinin and leupeptin (Fisher)/ml. Cells were incubated for 5 min at room temperature and then clarified by centrifugation at 14,000 × *g* for 10 min at 4°C. For each sample, 25 μg was separated by sodium dodecyl sulfate-polyacrylamide gel electrophoresis in a 4 to 20% acrylamide gradient gel, transferred to Immobilon P (Millipore), probed with an appropriate antibody, and detected by chemiluminescence using the West Pico substrate (Pierce). The antibody to the Myc epitope tag sequence was 9B11 from Cell Signaling. The antibody to α-tubulin was developed by J. Frankel and was obtained from the Developmental Studies Bank at the University of Iowa under the auspices of the National Institute of Child Health and Human Development. The polyclonal antibody to Erg11p was raised to the 15 amino-terminal amino acids of Erg11p and was used at a dilution of 1:1,000.

Reverse transcriptase PCR (RT-PCR). RNA was isolated from log-phase yeast cells by phenol-chloroform extraction as described elsewhere (www.microarrays.org). Following extraction and analysis by agarose gel, 6 μg of RNA was converted to cDNA by using SuperScript II reverse transcriptase (Invitrogen), according to the manufacturer's instructions. Following cDNA synthesis, the *ERG11* transcript was amplified using the primers *ERG11*+350F and *ERG11*+642R. The *SCS2* and *TUB1* transcripts were not altered by sterol pools and were used as controls for RNA loading. *SCS2* expression was analyzed using the primers *SCS2*+300F and *SCS2*+480R, and *TUB1* was analyzed using the primers *TUB1*+1F and *TUB1*+220R. The PCRs were prepared as a common pool and then divided into equal thirds in separate tubes. During the PCR, the tubes were removed at three different cycle numbers to ensure that the transcript was being monitored during the linear phase of the PCR. PCRs were separated on a 1.5% agarose 1000 gel (Invitrogen) and photographed.

RESULTS

Dap1p is a heme-1 domain protein that binds to heme. Dap1p is part of a widely conserved group of proteins that share sequence similarity with cytochrome b_5 (23), a heme-binding protein that activates multiple cytochrome P450 proteins (30). Because of the similarity between Dap1p and cytochrome b_5, we analyzed heme binding by Dap1p purified in *Escherichia coli*. When glutathione *S*-transferase fusion proteins with Dap1p were bound to glutathione-agarose columns, they had a brown appearance (data not shown), a characteristic of heme-binding proteins. Purified Dap1p was liberated from the column (Fig. 2A) and exhibited strong absorbance at 400 nm, indicating heme binding. Furthermore, when the reducing agent dithionate was added to Dap1p, the absorbance peak shifted to 420 nm (data not shown). We conclude that Dap1p binds to heme, like the related protein cytochrome b_5 and the Dap1p homologue IZAg (24).

Cytochrome b_5 binds to heme through a binding pocket composed of four α-helices (30). The sequences bridging these helices are highly conserved between cytochrome b_5 and the Dap1p-related proteins. We mutated the conserved residue of Dap1p, Asp91, to glycine and purified the Dap1p^{D91G} fusion protein. Like the wild-type protein, Dap1p^{D91G} was readily purified (Fig. 2A, lane 2), but Dap1p^{D91G}-containing agarose columns were not brown in color, and Dap1p^{D91G} exhibited no absorbance at 400 nm. Figure 2B shows the relative absorbances of Dap1p and Dap1p^{D91G}. Heme-binding measurements were performed in triplicate, and the difference in heme binding between Dap1p and Dap1p^{D91G} has been confirmed in multiple protein preparations. We conclude that the D91 residue is required for heme binding by Dap1p.

The D91G mutation within the Dap1p heme-1 domain inactivates Dap1p. To assess the biological importance of heme binding for Dap1p, we subcloned the wild-type *DAP1* and mutant *DAP1*^{D91G} genes into single-copy CEN plasmids for expression in yeast. The resulting plasmids were called *DAP1*-CEN and *DAP1*^{D91G}-CEN. Both plasmids were introduced into wild-type and *dap1*Δ yeast strains and tested for damage resistance. MMS had little effect on wild-type strains containing a control plasmid, *DAP1*-CEN, or *DAP1*^{D91G} (Fig. 2C, rows 7 to 9). In *dap1*Δ strains, cells containing the control plasmid were sensitive to MMS (Fig. 2C, row 10), while *DAP1*-CEN complemented the *dap1*Δ phenotype (Fig. 2C, row 11). In contrast, the *DAP1*^{D91G}-CEN plasmid was unable to complement the *dap1*Δ phenotype (Fig. 2C, row 12). We conclude that sequences within Dap1p that are required for heme binding are critical for Dap1p function in damage resistance.

MMS sensitivity in *dap1*Δ strains is suppressed by exogenous hemin. Next, we examined whether heme is the primary target for Dap1p or whether the heme-1 motif is a structural

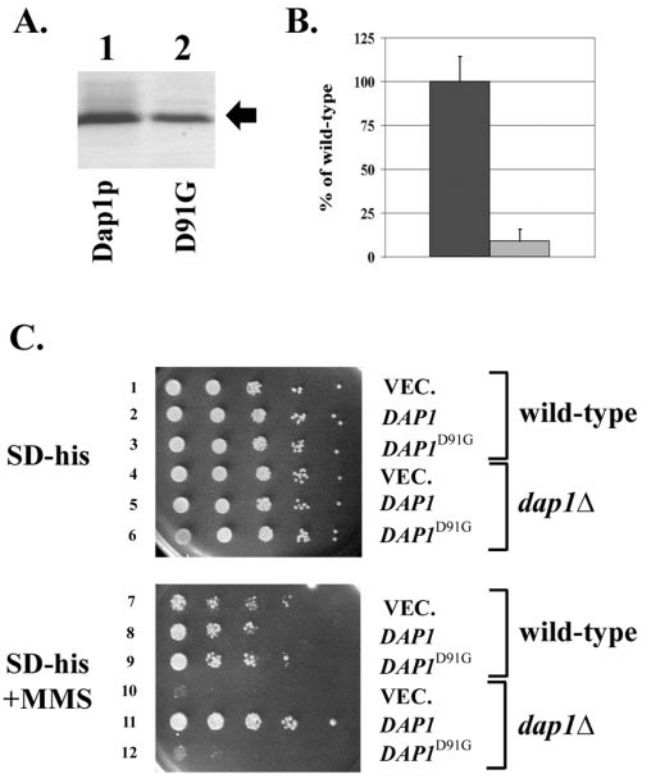

FIG. 2. Dap1p is a heme-binding protein, and heme binding is required for Dap1p-mediated damage resistance. (A) The highly conserved Asp91 residue of Dap1p was mutated to Gly, and wild-type Dap1p and Dap1p^{D91G} proteins were purified as fusion proteins with glutathione *S*-transferase. (B) Dap1p bound to heme (left bar), while the Dap1p^{D91G} lost heme-binding activity (right bar). (C) *DAP1* complements the *dap1*Δ phenotype, while *DAP1*^{D91G} does not. The entire *DAP1* open reading frame, along with 300 bp of promoter sequence, was subcloned in the single-copy plasmid pRS313, as was the *DAP1*^{D91G} mutant. Wild-type cells (rows 1 to 3 and 7 to 9) and *dap1*Δ strains (rows 4 to 6 and 10 to 12) were transformed with either a control plasmid (VEC., rows 1, 4, 7, and 10), a *DAP1*-containing plasmid (rows 2, 5, 8, and 11), or the *DAP1*^{D91G}-containing plasmid (rows 3, 6, 9, and 12). Cells were grown on medium lacking histidine to force retention of the plasmids. Growth was analyzed by spotting 10-fold dilutions on plates lacking histidine (top panel) or on the same plates containing 0.01% MMS (bottom panel).

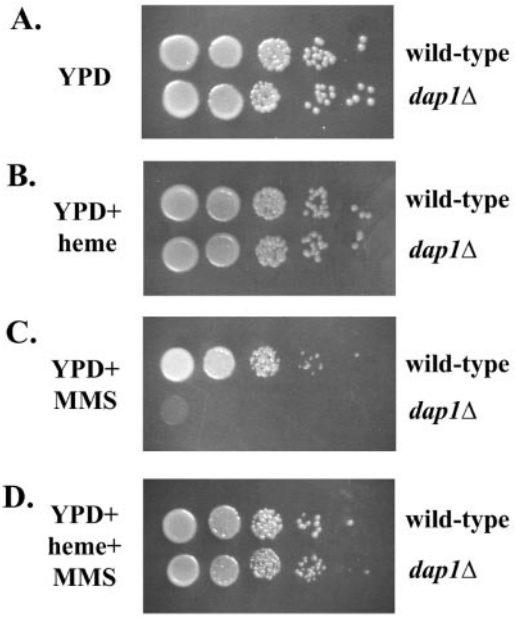

FIG. 3. MMS sensitivity in *dap1*Δ cells is suppressed by the addition of exogenous heme. Wild-type (RCY409-2a) and *dap1*Δ (RCY409-4b) cells were pregrown on YPD plates or YPD plates containing 13 μg of hemin/ml and then spotted on YPD plates (A), YPD plates containing 13 μg of hemin/ml (B), YPD plates containing 0.015% MMS (C), or YPD plates containing 13 μg of hemin/ml and 0.015% MMS (D). Pregrowth on hemin had no detectable effect on the growth of *dap1*Δ cells but suppressed MMS sensitivity in *dap1*Δ cells.

domain utilized by ligands other than heme, as suggested previously (23). We tested the model that heme binding is the target of Dap1p by adding exogenous hemin to wild-type and *dap1*Δ cells and then measuring MMS sensitivity.

To ensure uptake of hemin, wild-type and *dap1*Δ cells were maintained for approximately 50 generations on solid YPD medium, with or without hemin. Cells were then diluted and tested for growth on YPD, YPD containing hemin, YPD plus MMS, and YPD containing hemin plus MMS (Fig. 3). Pregrowth on solid YPD medium containing hemin suppressed MMS sensitivity in *dap1*Δ strains (Fig. 3C and D, bottom rows), while the growth of these strains was unaffected by hemin under normal conditions (Fig. 3B). As a control, we maintained a *dun1*Δ strain on similar plates containing hemin and measured MMS resistance. *DUN1* (damage uninducible) encodes a protein kinase that is required for signaling following DNA damage, and *dun1*Δ strains are damage sensitive (38). Growth on hemin had no effect on MMS resistance in the *dun1*Δ strain (data not shown), indicating that suppression of MMS sensitivity by heme is not a general property of damage resistance genes.

To quantitate the ability of hemin to suppress MMS sensitivity in *dap1*Δ strains, we measured the LD_{50} in *dap1*Δ strains before and after hemin addition. The LD_{50} is the dose of MMS at which 50% of the culture survives. As expected, *dap1*Δ cells had a lower LD_{50} value than wild-type cells (0.005% MMS versus 0.013%) (see Materials and Methods), and hemin suppressed MMS sensitivity in *dap1*Δ cells (0.005 versus 0.013%; $P = 0.00002$). We conclude that *dap1*Δ strains are deficient in MMS resistance because of defects in the targeting of heme to specific reactions or pathways.

Next, we examined sterol intermediates by gas chromatography in wild-type and *dap1*Δ cells in the absence and presence of hemin. Pregrowth in hemin had little effect on the accumulation of sterol intermediates in wild-type cells, except for a minor decrease in squalene concentrations (Fig. 4A and B). In *dap1*Δ cells grown on YPD, we detected elevated lanosterol, ergosta-5,7-dienol, episterol, and squalene levels (compare Figs. 4A and C), as observed in previous studies (14). While most of the sterol intermediates were detected as single peaks, ergosta-5,7-dienol coeluted closely with episterol and appeared as a shoulder on the episterol peak. Because of this overlapping elution profile, we have designated the episterol and ergosta-5,7-dienol peaks as a single peak. When *dap1*Δ cells were maintained on heme-containing plates, we detected decreased levels of lanosterol and squalene (compare Fig. 4C and D). We also detected elevated levels of zymosterol (Fig. 4C and D) and

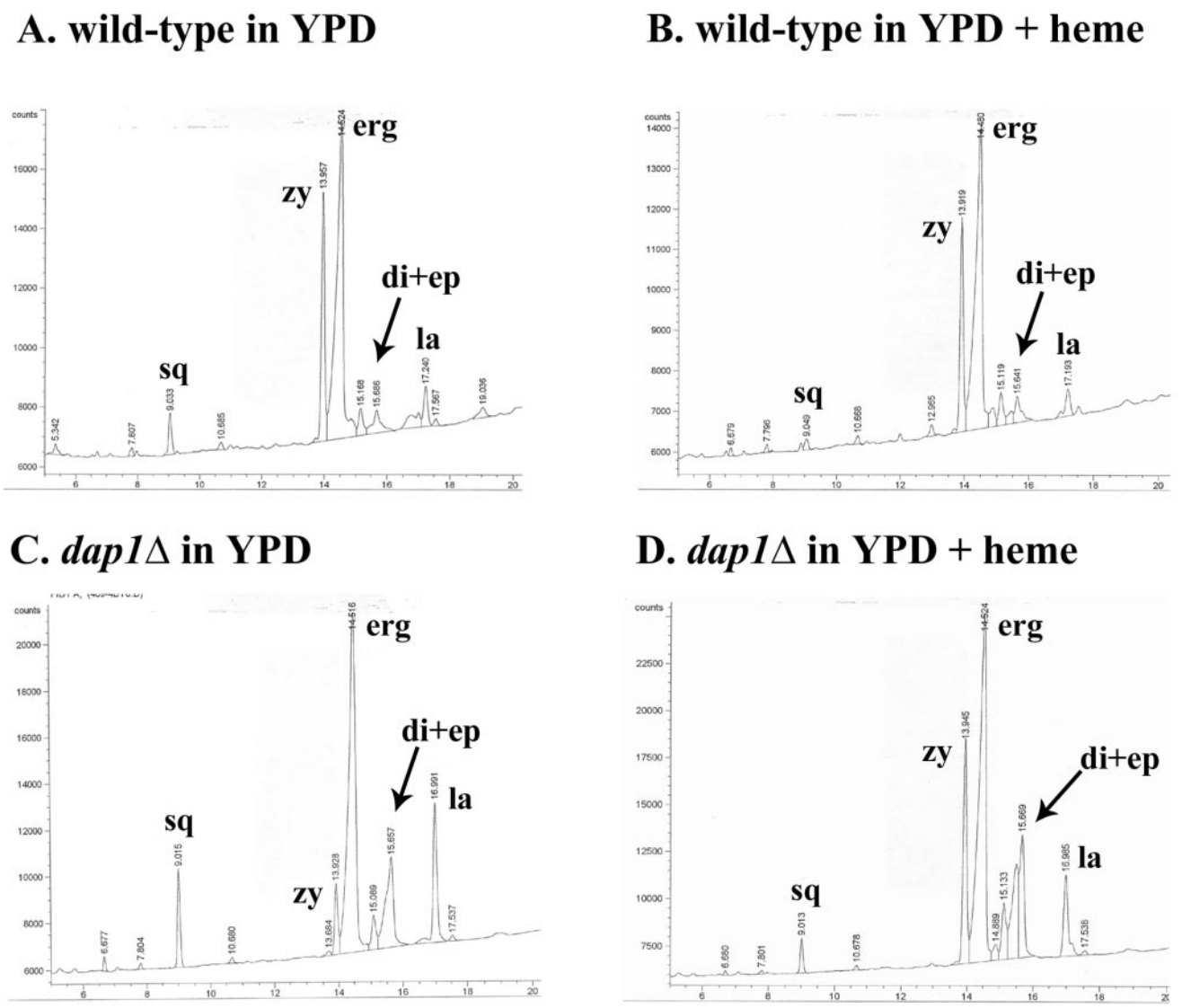

FIG. 4. Heme suppresses sterol synthetic defects in *dap1*Δ mutant strains. Wild-type (A and B) and *dap1*Δ (C and D) cells were maintained in YPD medium or in YPD supplemented with 39 μg of hemin/ml, and sterol intermediates were analyzed by gas chromatography. As previously noted, *dap1*Δ cells contain increased levels of lanosterol (la) and squalene (sq) relative to wild-type cells and decreased levels of zymosterol (zy) (compare panels A and C) (see also reference 14). The *dap1*Δ mutants also had increased levels of episterol and ergosta-5,7-dienol (di+ep). Growth in heme-containing medium caused a decrease in squalene and lanosterol in *dap1*Δ cells (D) and an increase in zymosterol. Similar changes were observed in cells maintained in 13 μg of hemin/ml.

modest increases in ergosta-5,7-dienol and episterol (Fig. 4C and D), sterol intermediates that are downstream of lanosterol (Fig. 1). These findings indicate that Erg11p/Cyp51p/lanosterol demethylase function is attenuated in *dap1*Δ mutants and is partially restored by the addition of heme.

***ERG11* is a multicopy suppressor of sterol biosynthesis and damage sensitivity in *dap1*Δ mutants.** In some cases, overexpression of a downstream component of a genetic pathway is capable of suppressing a mutation in an upstream gene (13). For that reason, we tested the hypothesis that multiple copies of *ERG11* would suppress *dap1*Δ phenotypes. The entire *ERG11* open reading frame, along with 300 bp of upstream promoter sequence, was cloned into the multiple-copy plasmid YEp*lac*195, resulting in the plasmid YEp-*ERG11.* Wild-type or *dap1*Δ mutants expressing the *ERG11* plasmid did not have altered growth under normal conditions (Fig. 5A, upper panel, rows 2 and 4). In contrast, YEp-*ERG11* completely suppressed the sensitivity of *dap1*Δ mutants to the antifungal agent itraconazole, a clinical Erg11p inhibitor (Fig. 5A, middle panel, compare rows 3 and 4). YEp-*ERG11* also increased itraconazole resistance in wild-type cells (Fig. 5A, middle panel, rows 1 and 2). The result is consistent with Erg11p acting downstream of Dap1p in conferring itraconazole resistance.

In addition to suppressing itraconazole sensitivity, YEp-*ERG11* suppressed the partial ergosterol synthetic defect in *dap1*Δ cells. Gas chromatographic analysis of wild-type and *dap1*Δ strains harboring YEp*lac*195 demonstrated elevated levels of squalene and lanosterol and decreased levels of zy-

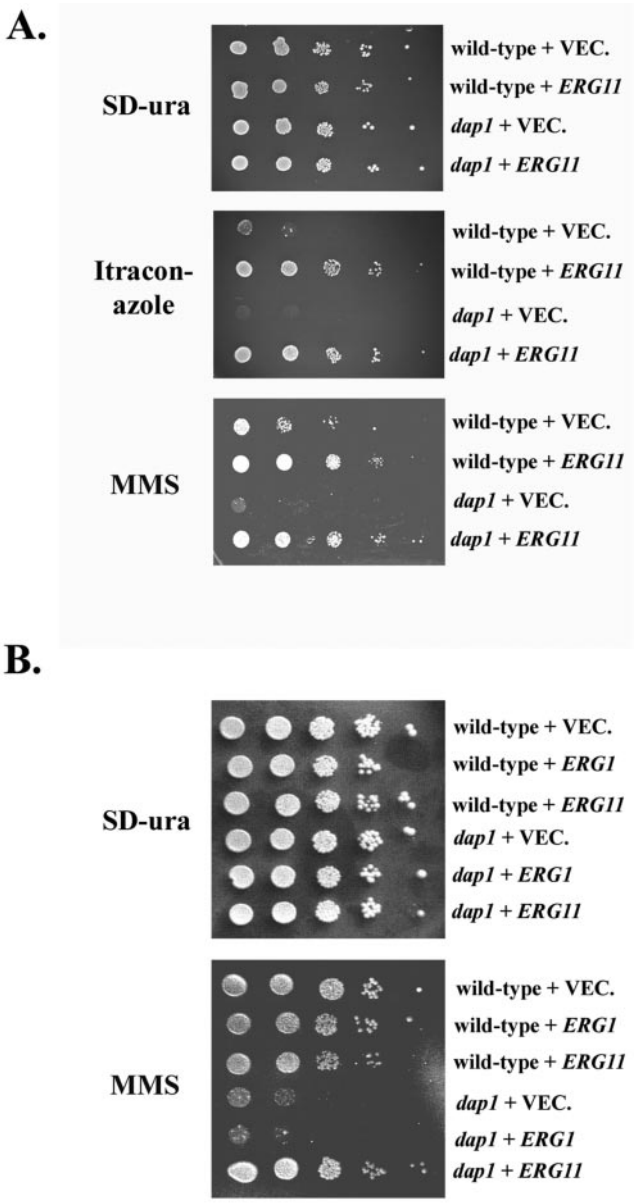

FIG. 5. Multiple copies of *ERG11*/lanosterol demethylase, but not *ERG1*/squalene epoxidase, suppress sensitivity of *dap1*Δ mutants to azole inhibitors and MMS-induced damage. (A) Log-phase cells were serially diluted 1:10 and spotted onto plates containing synthetic medium lacking uracil (upper panel), the same medium overlaid with 0.2 mg of itraconazole/ml (middle panel), or the same medium containing 0.015% MMS (lower panel). The strains tested were RCY432 (the wild-type strain RCY409-2a harboring the plasmid YEp*lac*195 [wild-type + YEp]), RCY433 (RCY409-2a harboring the *ERG11* multiple copy plasmid pRH4 [wild-type + YEp-*ERG11*]), RCY434 (the *dap1*Δ strain RCY409-4b harboring the plasmid YEplac195 [*dap1*Δ + YEp]), and RCY435 (RCY409-4b harboring pRH4 [*dap1*Δ + YEp-*ERG11*]). Multiple copies of *ERG11* had little effect on normal growth of wild-type or *dap1*Δ strains on SD-ura (upper panel). As expected, *dap1*Δ strains harboring YEp*lac*195 were sensitive to itraconazole and MMS (middle and lower panels, third rows). Multiple copies of *ERG11* suppressed the sensitivity of *dap1*Δ strains to itraconazole and MMS (middle and lower panels, fourth rows). (B) Cells were grown, spotted, and diluted similarly to those shown in panel A. The strains tested were RCY409-2a/wild-type cells harboring the control plasmid YEp*lac*195 (rows 1, wild-type + VEC.), the *ERG1* multicopy plasmid pJM60 (rows 2, wild-type + YEp-*ERG1*), and the *ERG11* multicopy plasmid pRH4 (rows 3, wild-type + *ERG11*), and the RCY409-4b/*dap1*Δ strain harboring the control plasmid YEp*lac*195 (rows 4, *dap1* + VEC.), the *ERG1* multicopy plasmid pJM60 (rows 5, *dap1* + Yep-*ERG1*), and the *ERG11* multicopy plasmid pRH4 (rows 6, *dap1* + *ERG11*). While multiple copies of *ERG11* suppressed MMS sensitivity in *dap1*Δ cells, multiple copies of *ERG1* did not.

mosterol in *dap1*Δ cells (Fig. 6, compare panels A and C), as expected from previous experiments (14). As noted for Fig. 4, we detected elevated levels of episterol and ergosta-5,7-dienol in *dap1*Δ mutants, suggesting a defect in the reaction catalyzed by Erg5p. The YEp-*ERG11* plasmid did not have a marked effect on sterol synthesis in wild-type cells, although there was a detectable increase in squalene (Fig. 6, compare panels A and B). In contrast, YEp-*ERG11* led to profound changes in sterol levels in *dap1*Δ cells, with levels of zymosterol and lanosterol resembling those in wild-type cells (Fig. 6D). YEp-*ERG11* also led to an elevated accumulation of episterol and ergosta-5,7-dienol, further suggesting defective Erg3p and Erg5p function in *dap1*Δ cells.

Because YEp-*ERG11* restored sterol biosynthesis in *dap1*Δ cells, we examined the effect of YEp-*ERG11* on damage resistance. We compared growth of *dap1*Δ mutants harboring YEp*lac*195 and YEp-*ERG11* on plates containing 0.015% MMS. YEp-*ERG11* completely suppressed MMS resistance in *dap1*Δ mutants, while the same strain harboring YEp*lac*195 (Fig. 5, VEC) was sensitive to the drug (Fig. 5A, lower panel, compare rows 3 and 4). Furthermore, the LD_{50} of MMS was significantly different in *dap1*Δ cells containing the YEp*lac*195 and YEp-*ERG11* plasmids (0.005 versus 0.018% MMS; $P = 0.0008$). Similar to the itraconazole sensitivity assay, YEp-*ERG11* also caused a slight increase in MMS resistance in wild-type cells (Fig. 5A, lower panel, rows 1 and 2). We conclude that *ERG11* is an efficient multicopy suppressor of damage sensitivity and sterol synthetic defects in *dap1*Δ mutants.

***ERG1*, *ERG5*, and *CYB5* are not multicopy suppressors of *dap1*Δ damage sensitivity.** Sterol synthesis profiles suggested that Erg1p and Erg5p may require Dap1p, because elevated levels of their substrates were detected in *dap1*Δ mutants (Fig. 4 and 6) (14). We cloned *ERG1* and *ERG5* into a multicopy plasmid, YEp*lac*195, forming the plasmids YEp-*ERG1* and YEp-*ERG5*, and introduced the plasmids into wild-type and *dap1*Δ strains. Unlike *ERG11*, multiple copies of *ERG1* and *ERG5* did not confer MMS resistance to *dap1*Δ cells (Fig. 5B, lower panel, fifth row, and data not shown). *ERG1* overexpression suppressed the accumulation of squalene in *dap1*Δ cells (data not shown) but did not affect lanosterol accumulation, as expected from the order of the ergosterol synthetic pathway (Fig. 1). We conclude that Erg1p and Erg5p are not targets for Dap1p in MMS resistance.

Dap1p shares a heme-binding domain with the *CYB5*/cytochrome b_5 protein (23). Like Dap1p, Cyb5p regulates resistance to azole antifungal agents (33), possibly because Cyb5p and Cyb5p reductase can substitute for the Erg11p reductase Ncp1p (20). Unlike *ERG11*, multiple copies of *CYB5* did not suppress MMS or azole sensitivity in *dap1*Δ mutant cells (data not shown). We conclude that Dap1p and Cyb5p do not have redundant functions in MMS resistance.

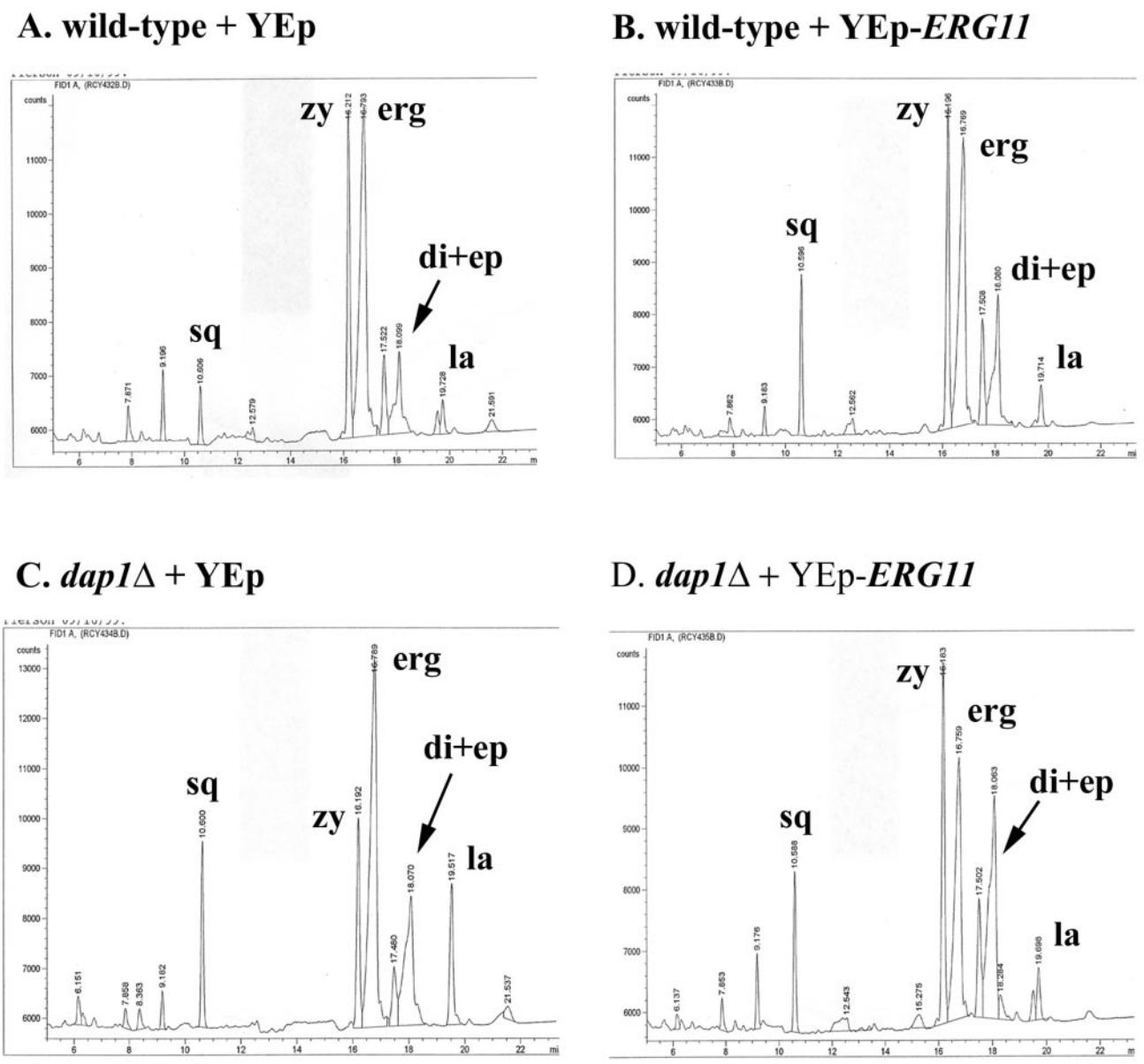

FIG. 6. Multiple copies of *ERG11* suppress sterol synthetic defects in *dap1*Δ mutant cells. The levels of sterol synthetic intermediates in four yeast strains were measured by gas chromatography. (A and B) Wild-type cells harboring either a control plasmid (A) or the multicopy *ERG11* plasmid YEp-*ERG11* (B) contained normal levels of sterol synthetic intermediates. However, we note that *ERG11* overexpression caused a marked accumulation of squalene (B). (C) Cells lacking Dap1p contained elevated levels of lanosterol, ergosta-5,7-dienol, episterol, and squalene. (D) Overexpression of *ERG11* decreased the levels of lanosterol in *dap1*Δ cells but caused an increase in the lanosterol metabolites ergosta-5,7-dienol, episterol, and zymosterol. The elevated levels of squalene observed in *dap1*Δ cells (C) (14) were unaffected by *ERG11* overexpression (D).

Multiple copies of *ERG11* do not suppress damage sensitivity in checkpoint mutants or sterol biosynthesis mutants downstream of *ERG11*. We examined the ability of the multicopy YEp-*ERG11* plasmid to suppress MMS sensitivity in strains lacking the damage checkpoint proteins *MEC1* (1, 36) and *DUN1* (38). Strains harboring the *mec1-21* and *dun1*Δ mutations are sensitive to MMS, and MMS sensitivity was not restored by *ERG11* overexpression in these strains (data not shown). Thus, *ERG11* is not a general suppressor of damage-sensitive mutants. Next, we examined the ability of YEp-*ERG11* to suppress additional lesions in the sterol biosynthetic pathway. As expected from the work of other labs, *erg2*Δ mutants are sensitive to MMS (3), and we found that *ERG11* overexpression did not suppress MMS sensitivity in *erg2*Δ strains (data not shown). Our results suggest that *ERG11* suppresses damage sensitivity through the ergosterol synthetic pathway.

Dap1p is required for maintenance of Erg11p levels. The transcription of *ERG11* is altered in response to oxygen, glucose, and heme (7). We analyzed the transcription of the *ERG11* gene by RT-PCR in wild-type and *dap1*Δ cells to determine the extent to which Dap1p regulates *ERG11* transcrip-

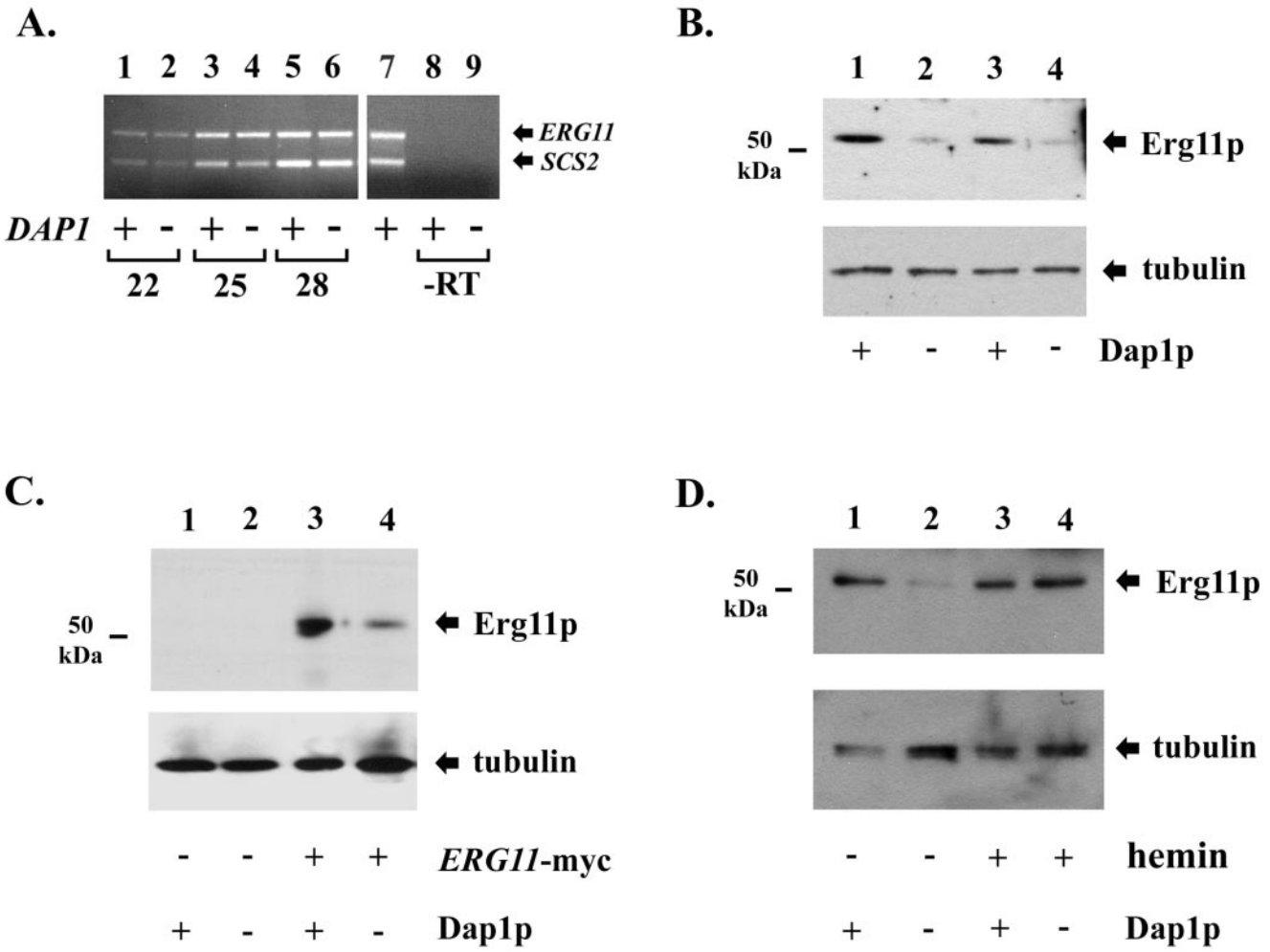

FIG. 7. Dap1p is required for expression of the Erg11p protein. (A) Dap1p does not regulate *ERG11* transcription. RNA was isolated from the strains RCY409-2a/wild type (lanes 1, 3, 5, 7, and 8) and RCY409-4b/*dap1*Δ (lanes 2, 4, 6, and 9) and reverse transcribed. *ERG11* expression was analyzed by RT-PCR (upper band) with *SCS2* gene transcription as a control for loading (lower panel). To ensure that samples were analyzed in the linear phase of the reaction, samples were withdrawn at 22, 25, and 28 cycles of the PCR. To control against PCR products arising from contaminating genomic DNA in the sample, parallel reactions in which RT was omitted from the reaction mixture were analyzed using the same procedure for 28 cycles of PCR. Lane 7 is identical to lane 8, but RT was added. (B) Two pairs of wild-type and *dap1*Δ strains from different genetic crosses were lysed, and expression of the Erg11p protein was analyzed by Western blotting. The strains RCY409-2a (lane 1), RCY-409-4b (lane 2), RCY407-12d (lane 3), and RCY407-1d (lane 4) were analyzed for Erg11p (upper panel) or tubulin as a loading control (lower panel). The presence of Dap1p in the strains is indicated, and the migration of a molecular mass marker is on the left side of the upper panel. Erg11p was decreased by 5.0- and 3.1-fold in the two *dap1*Δ strains compared to wild type. (C) The Erg11p open reading frame was cloned in frame with the myc epitope tag sequence on a single-copy plasmid, and wild-type (lanes 1 and 3) and *dap1*Δ (lanes 2 and 4) strains were transformed with either a control plasmid (lanes 1 and 2) or the Erg11p-myc-containing plasmid (lanes 3 and 4). The strains were lysed and analyzed by Western blotting with antibodies to myc (upper panel) and tubulin (lower panel). (D) Expression levels of Erg11p (top panel) or the loading control tubulin (bottom panel) were analyzed by Western blotting. The wild type (lanes 1 and 3) and *dap1*Δ strains (lanes 2 and 4) RCY409-2a and RCY409-4b, respectively, were grown in YPD medium (lanes 1 and 2) or YPD medium containing 13 μg of heme/ml for 1 h and then lysed and analyzed. Erg11p expression was decreased approximately fourfold in *dap1*Δ cells grown in YPD, while addition of heme restored Erg11p expression to wild-type levels (compare lanes 2 and 4).

tion. We used two different genes, *SCS2* and *TUB1*, as controls for loading and analyzed *ERG11* expression at multiple PCR cycles (Fig. 7A). The analysis was performed in triplicate. We conclude that *DAP1* does not significantly alter *ERG11* transcription.

Next, we analyzed protein samples from wild-type and *dap1*Δ strains by using an anti-Erg11p antibody. Erg11p levels were decreased approximately fourfold in *dap1*Δ haploid strains compared to matched wild-type strains from two separate genetic crosses (Fig. 7B, upper panel; lanes 1 and 3 contain proteins from wild-type cells and lanes 2 and 4 contain proteins from *dap1*Δ cells). In addition, a wild-type diploid strain had markedly higher Erg11p levels than a *dap1*Δ diploid strain constructed from progeny from the same genetic cross (data not shown).

To ensure that our assignment of the 55-kDa band to Erg11p was correct, we prepared a single-copy (CEN) plasmid containing the *ERG11* open reading frame fused to the myc

epitope tag and introduced this plasmid into wild-type and *dap1*Δ strains. As expected, Erg11p-myc migrated as a single 55-kDa band that was detected only in strains harboring the appropriate plasmid (Fig. 7C, upper panel, compare lanes 3 and 4 to control strains in lanes 1 and 2). Wild-type strains expressed Erg11p-myc at approximately fourfold-higher levels than a *dap1*Δ strain (Fig. 7C, upper panel, lanes 3 and 4), similar to the result shown in Fig. 7B. We conclude that Dap1p is required for wild-type expression levels of Erg11p.

Both addition of heme and *ERG11* overexpression suppress MMS sensitivity in *dap1*Δ cells (Fig. 3 and 5). We examined whether heme addition affected Erg11p stability in *dap1*Δ cells by Western blotting with the anti-Erg11p antibody. As noted in Fig. 7B, Erg11p was expressed at lower levels in *dap1*Δ cells than in comparable wild-type cells (Fig. 7D, lanes 1 and 2). By growing the same cells in 13 μg of heme/ml for 1 h, we detected a sharp increase in Erg11p stability in *dap1*Δ cells (Fig. 7D, compare lanes 2 and 4). Our results are consistent with a model in which heme suppresses MMS sensitivity in *dap1*Δ cells by stabilizing Erg11p. However, we have not excluded the possibility that heme may alter the stability of proteins other than Erg11p.

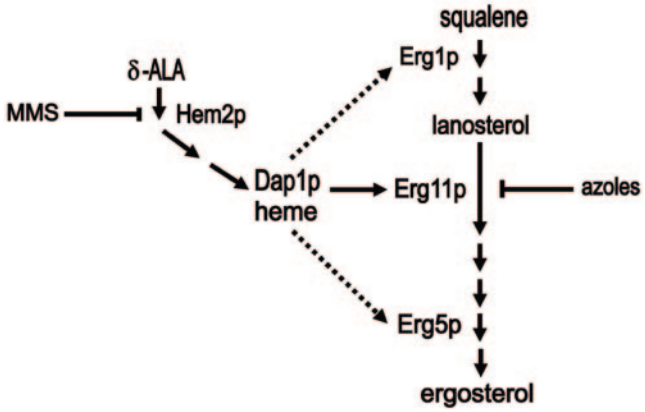

FIG. 8. Placement of Dap1p in the ergosterol biosynthetic pathway. Dap1p functions as an upstream regulator of Erg11p (solid arrow), regulating the stability of Erg11p. Dap1p also regulates the Erg1p protein (dashed arrow), although this does not contribute to MMS resistance. Dap1p also has a minor role in regulating Erg3p and Erg5p, because the Erg3p substrate episterol and Erg5p substrate ergosta-5,7-dienol are elevated in *dap1*Δ cells (Fig. 4C), particularly following *ERG11* overexpression (Fig. 6D). The heme biosynthetic pathway acts upstream of Dap1p, and *dap1*Δ phenotypes are suppressed by addition of exogenous heme. One possible explanation for this order is that Lum et al. (21) have identified Hem1p and Hem2p as molecular targets for MMS (left of figure).

DISCUSSION

Dap1p and its relatives share homology with cytochrome b_5 (23), a heme-binding protein (30). We have shown that Dap1p binds to heme and that Dap1p regulates the cytochrome P450 protein Erg11p/Cyp51p. Dap1p homologues are expressed in the liver (8, 22, 29, 31), where their proposed role is to activate the cytochrome P450 protein Cyp21, elevating the oxidation of progesterone (24). However, the previous study relied on an artificial overexpression system (24), and the present work is the first demonstration of an in vivo function for a Dap1p family member in regulating a P450 protein.

We propose a model for the Dap1p pathway in which Dap1p acts upstream of Erg11p by stabilizing Erg11p (Fig. 8). Aberrant sterol profiles in *dap1*Δ cells also suggest a role for Dap1p in activating Erg1p, Erg3p, and Erg5p (Fig. 4, 6, and 8) (14). Erg11p, Erg1p/squalene epoxidase, and Erg5p/sterol C-22 desaturase (a cytochrome P450 protein) require a cytochrome P450 reductase, but only *ERG11* overexpression suppressed MMS sensitivity in *dap1*Δ cells. Thus, we found no evidence that Erg1p or Erg5p mediate MMS resistance by acting downstream of Dap1p. However, our data do not exclude a role for Dap1p in regulating Erg1p or Erg5p in the absence of MMS. The mechanism through which Dap1p regulates Erg3p/sterol C-5 desaturase is unclear.

Our results support a model in which heme binding by Dap1p is required to stabilize Erg11p (Fig. 8). Erg11p binds to heme, and Dap1p could increase the stability of the Erg11p-heme complex. By this model, loss of Dap1p would destabilize the Erg11p-heme complex, triggering Erg11p degradation. The model predicts that loss of Dap1p could be suppressed by higher than normal levels of either Erg11p or heme, which were the observed results (Fig. 3 and 5). We tested the possibility that Dap1p stabilizes Erg11p by binding directly to Erg11p, but we were unable to detect a Dap1p-Erg11p complex by immunoprecipitation (data not shown). However, our results do not exclude the possibility of a transient Dap1p-Erg11p interaction that is not detectable by immunoprecipitation. Mass genomic screens have failed to detect any direct binding partners for Erg11p (16), even known Erg11p regulators such as Ncp1p (35) and Cyb5p (20), suggesting that Erg11p complexes may be unstable under the widely used lysis and precipitation conditions.

Our data suggest that the heme biosynthetic pathway regulates Dap1p and directs its functions in sterol biosynthesis and MMS resistance. The early stages of heme biosynthesis are catalyzed by Hem1p/δ-aminolevulinate synthase and Hem2p/δ-aminolevulinate dehydratase (Fig. 8). Our results are consistent with Hem2p acting upstream of Dap1p, because *dap1*Δ phenotypes can be restored by exogenous heme (Fig. 3 and 4) but not by the Hem2p substrate δ-aminolevulinic acid (data not shown). Lum and colleagues have identified Hem1p and Hem2p as potential targets for MMS, because *HEM1*/*hem1* and *HEM2*/*hem2* diploid strains are preferentially selected from populations of MMS-treated cells (21). If Hem1p and Hem2p are inhibited by MMS, heme synthesis would likely be lost following MMS treatment, depleting Dap1p and Erg11p of heme, triggering Erg11p degradation. In support of this model, supplementing *dap1*Δ cells with exogenous heme suppressed MMS sensitivity (Fig. 3) and increased Erg11p stability (Fig. 7).

Our data are consistent with a scenario in which ergosterol or a sterol intermediate is directly modified by MMS. Ergosterol has multiple roles in yeast, regulating cell cycle progression, oxygen sensing, intracellular transport, and membrane fluidity (7). If ergosterol were methylated by MMS, the modified sterol could become aberrantly localized or degraded and Erg11p would be required for restoring normal sterol pools. Because *dap1*Δ cells have decreased Erg11p levels, ergosterol synthesis would be disrupted, potentially arresting the cell cy-

cle. We have previously reported cell cycle arrest in *dap1*Δ cells treated with MMS (14), which is consistent with this model.

A variation of this model is that Erg11p could act directly on methylated sterols. Erg11p is a cytochrome P450 protein, and the majority of cytochrome P450 proteins have multiple substrates (27, 37). Indeed, some human cytochrome P450 proteins modify steroid hormones and oxidize numerous drugs. In yeast, there is a precedent for a cytochrome P450 protein functioning in sterol synthesis and xenobiotic metabolism. Erg5p/sterol C-22 desaturase catalyzes the conversion of ergosta-5,7,24(28)-trienol to ergosta-5,7,22,24(28)-tetraenol in the sterol biosynthetic pathway (reviewed in reference 7). Erg5p also catalyzes the conversion of benzo[*a*]pyrene to 3-hydroxybenzo[*a*]pyrene (18). Benzo[*a*]pyrene is a polycyclic aromatic hydrocarbon that is a carcinogen arising from incomplete hydrocarbon combustion, and 3-hydroxybenzo[*a*]pyrene is a hydrophilic derivative. Although Erg5p provides a precedent for yeast P450 proteins catalyzing lipid synthesis and xenobiotic metabolism, we note that lanosterol is the only known Erg11p substrate.

In conclusion, we have delineated a novel pathway that regulates resistance to a widely used alkylating agent. The proteins that mediate resistance to alkylating agents are important in cancer therapeutics, because the alkylating agents cyclophosphamide, dacarbazine, procarbozine, streptozotocin, and busulfan are used in cancer chemotherapy for lymphoma, melanoma, and pancreatic tumors (15). Our findings implicate Dap1p, Erg11p, and heme in resistance to alkylating agents in yeast. It is likely that mammalian homologues share some features of the Dap1p pathway, suggesting a novel mode of regulating diverse pathways for sterol synthesis and xenobiotic metabolism.

ACKNOWLEDGMENTS

We are grateful to Randal Hand at the University of North Carolina at Chapel Hill for technical assistance and Todd Porter at the University of Kentucky for helpful suggestions on measuring heme binding. We are also grateful to Jasper Rine's laboratory for the yeast strain JRY7187.

This work was paid for in part by the University of Kentucky Medical Center start-up funds and by NIH grant COBRE P20 RR 15592. M.B. acknowledges support of NIH grant GM62104.

REFERENCES

1. **Allen, J. B., Z. Zhou, W. Siede, E. C. Friedberg, and S. J. Elledge.** 1994. The *SAD1/RAD53* protein kinase controls multiple checkpoints and DNA damage-induced transcription in yeast. Genes Dev. **8:**2416–2428.
2. **Bard, M., N. D. Lees, L. S. Burrows, and F. W. Kleinhaus.** 1978. Differences in crystal violet uptake and cation-induced death among yeast sterol mutants. J. Bacteriol. **135:**1146–1148.
3. **Begley, T. J., A. S. Rosenbach, T. Ideker, and L. D. Samson.** 2002. Damage recovery pathways in *Saccharomyces cerevisiae* revealed by genomic phenotyping and interactome mapping. Mol. Cancer Res. **1:**103–112.
4. **Bennett, C. B., L. K. Lewis, G. Karthikeyan, K. S. Lobachev, Y. H. Jin, J. F. Sterling, J. R. Snipe, and M. A. Resnick.** 2001. Genes required for ionizing radiation resistance in yeast. Nat. Genet. **29:**426–434.
5. **Chang, M., M. Bellaoui, C. Boone, and G. W. Brown.** 2002. A genome-wide screen for methyl methanesulfonate-sensitive mutants reveals genes required for S phase progression in the presence of DNA damage. Proc. Natl. Acad. Sci. USA **99:**16934–16939.
6. **Craven, R. J., and T. D. Petes.** 2001. The *Saccharomyces cerevisiae* suppressor of choline sensitivity (*SCS2*) gene is a multicopy suppressor of *mec1* telomeric silencing defects. Genetics **158:**145–154.
7. **Daum, G., N. D. Lees, M. Bard, and R. Dickson.** 1998. Biochemistry, cell biology, and molecular biology of lipids of *Saccharomyces cerevisiae*. Yeast **14:**1471–1510.
8. **Falkenstein, E., C. Meyer, C. Eisen, P. C. Scriba, and M. Wehling.** 1996. Full-length cDNA sequence of a progesterone membrane-binding protein from vascular smooth muscle cells. Biochem. Biophys. Res. Commun. **229:**86–89.
9. **Game, J. C.** 2000. The *Saccharomyces* repair genes at the end of the century. Mutat. Res. **451:**277–293.
10. **Gasch, A. P., M. Huang, S. Metzner, D. Botstein, S. J. Elledge, and P. O. Brown.** 2001. Genomic expression responses to DNA-damaging agents and the regulatory role of the yeast ATR homolog Mec1p. Mol. Biol. Cell **12:**2987–3003.
11. **Gerdes, D., M. Wehling, B. Leube, and E. Falkenstein.** 1998. Cloning and tissue expression of two putative steroid membrane receptors. Biol. Chem. **379:**907–911.
12. **Gietz, R. D., and A. Sugino.** 1988. New yeast-*Escherichia coli* shuttle vectors constructed with in vitro mutagenized yeast genes lacking six-base pair restriction sites. Gene **74:**527–534.
13. **Guthrie, C., and G. R. Fink (ed.).** 1991. Guide to yeast genetics and molecular biology. Academic Press, San Diego, Calif.
14. **Hand, R. A., N. Jia, M. Bard, and R. J. Craven.** 2003. *Saccharomyces cerevisiae* Dap1p, a novel DNA damage response protein related to the mammalian membrane-associated progesterone receptor. Eukaryot. Cell **2:**306–317.
15. **Hardman, J. G., and L. E. Limbird (ed.).** 2001. Goodman & Gilman's the pharmacological basis of therapeutics. McGraw-Hill, New York, N.Y.
16. **Ho, Y., A. Gruhler, A. Heilbut, G. D. Bader, L. Moore, S. L. Adams, A. Millar, P. Taylor, K. Bennett, K. Boutilier, L. Yang, C. Wolting, I. Donaldson, S. Schandorff, J. Shewnarane, M. Vo, J. Taggart, M. Goudreault, B. Muskat, C. Alfarano, D. Dewar, Z. Lin, K. Michalickova, A. R. Willems, H. Sassi, P. A. Nielsen, K. J. Rasmussen, J. R. Andersen, L. E. Johansen, L. H. Hansen, H. Jespersen, A. Podtelejnikov, E. Nielsen, J. Crawford, V. Poulsen, B. D. Sorensen, J. Matthiesen, R. C. Hendrickson, F. Gleeson, T. Pawson, M. F. Moran, D. Durocher, M. Mann, C. W. Hogue, D. Figeys, and M. Tyers.** 2002. Systematic identification of protein complexes in *Saccharomyces cerevisiae* by mass spectrometry. Nature **415:**180–183.
17. **Jelinsky, J. A., and L. D. Samson.** 1999. Global response of *Saccharomyces cerevisiae* to an alkylating agent. Proc. Natl. Acad. Sci. USA **96:**1486–1491.
18. **Kelly, S. L., D. C. Lamb, and D. E. Kelly.** 1997. Sterol 22-desaturase, cytochrome P45061, possesses activity in xenobiotic metabolism. FEBS Lett. **412:**233–235.
19. **Krebs, C. J., E. D. Jarvis, J. Chan, J. P. Lydon, S. Ogawa, and D. W. Pfaff.** 2000. A membrane-associated progesterone-binding protein, 25-Dx, is regulated by progesterone in brain regions involved in female reproductive behaviors. Proc. Natl. Acad. Sci. USA **97:**12816–12821.
20. **Lamb, D. C., D. E. Kelly, N. J. Manning, M. A. Kaderbhai, and S. L. Kelly.** 1999. Biodiversity of the P450 catalytic cycle: yeast cytochrome b_5/NADH cytochrome b_5 reductase complex efficiently drives the entire sterol 14-demethylation (CYP51) reaction. FEBS Lett. **462:**283–288.
21. **Lum, P. Y., C. D. Armour, S. B. Stepaniants, G. Cavet, M. K. Wolf, J. S. Butler, J. C. Hinshaw, P. Garnier, G. D. Prestwich, C. J. Roberts, and D. D. Shoemaker.** 2004. Discovering modes of action for therapeutic compounds using a genome-wide screen of yeast heterozygotes. Cell **116:**121–137.
22. **Meyer, C., R. Schmid, P. C. Scriba, and M. Wehling.** 1996. Purification and partial sequencing of high-affinity progesterone binding sites from porcine liver membranes. Eur. J. Biochem. **239:**726–731.
23. **Mifsud, W., and A. Bateman.** 2002. Membrane-bound progesterone receptors contain a cytochrome b_5-like ligand-binding domain. Genome Biol. **3:**1–5.
24. **Min, L., H. Takemori, Y. Nonaka, Y. Katoh, J. Doi, N. Horike, H. Osamu, F. S. Raza, G. P. Vinson, and M. Okamoto.** 2004. Characterization of the adrenal-specific antigen IZA (inner zone antigen) and its role in steroidogenesis. Mol. Cell. Endocrinol. **215:**143–148.
25. **Molzahn, S. W., and R. A. Woods.** 1972. Polyene resistance and the isolation of sterol mutants in *Saccharomyces cerevisiae*. J. Gen. Microbiol. **72:**339–348.
26. **Myung, K., and R. D. Kolodner.** 2002. Suppression of genome instability by redundant S-phase checkpoint pathways in *Saccharomyces cerevisiae*. Proc. Natl. Acad. Sci. USA **99:**4500–4507.
27. **Nebert, D. W., and D. W. Russell.** 2002. Clinical importance of the cytochromes P450. Lancet **360:**1155–1162.
28. **Prakash, S., and L. Prakash.** 1977. Increased spontaneous mitotic segregation in MMS-sensitive mutants of *Saccharomyces cerevisiae*. Genetics **87:**229–236.
29. **Raza, F. S., H. Takemori, H. Tojo, M. Okamoto, and G. P. Vinson.** 2001. Identification of the rat adrenal zona fasciculate/reticularis specific protein, inner zone antigen (IZAg), as the putative membrane progesterone receptor. Eur. J. Biochem. **268:**2141–2147.
30. **Schenkman, J. B., and I. Janssen.** 2003. The many roles of cytochrome b_5. Pharm. Ther. **97:**139–152.
31. **Selmin, O., G. W. Lucier, G. C. Clark, A. M. Tritscher, J. P. Vanden Heuvel, J. A. Gastel, N. J. Walker, T. R. Sutter, and D. A. Bell.** 1996. Isolation and characterization of a novel gene induced by 2,3,7,8-tetrachlorodibenzo-*p*-dioxin in rat liver. Carcinogenesis **17:**2609–2615.
32. **Thomas, B. J., and R. Rothstein.** 1989. Elevated recombination rates in transcriptionally active DNA. Cell **56:**619–630.
33. **Truan, G., J. C. Epinat, C. Rougeulle, C. Cullin, and D. Pompon.** 1994. Cloning and characterization of a yeast cytochrome b_5-encoding gene which suppresses ketoconazole hypersensitivity in a NADPH-P450 reductase-deficient strain. Gene **142:**123–127.
34. **Vanden Bosshe, H. G., G. Willemsens, W. Cools, P. Marichal, and W.**

Lauwers. 1983. Hypothesis on the molecular basis of the antifungal activation of the N-substituted imidazoles and triazoles. Biochem. Soc. Trans. **11:**665–667.

35. **Venkateswarlu, K., D. C. Lamb, D. E. Kelly, N. J. Manning, and S. L. Kelly.** 1998. The N-terminal membrane domain of yeast NADPH-cytochrome P450 (CYP) oxidoreductase is not required for catalytic activity in sterol biosynthesis or in reconstitution of CYP activity. J. Biol. Chem. **273:**4492–4496.
36. **Weinert, T. A., G. L. Kiser, and L. H. Hartwell.** 1994. Mitotic checkpoint genes in budding yeast and the dependence of mitosis on DNA replication and repair. Genes Dev. **8:**652–665.
37. **Werck-Reichart, D., and R. Feyereisen.** 2000. Cytochromes P450: a success story. Genome Biol. **6:**1–9.
38. **Zhou, Z., and S. J. Elledge.** 1993. *DUN1* encodes a protein kinase that controls the DNA damage response in yeast. Cell **75:**1119–1127.